Supporting Information

(1) The bulk structures of marcasite- and pyrite-type NiS_2

The marcasite-type bulk NiS_2 [Fig. S1(a)] has an orthorhombic lattice in $Pnnm$ symmetry with two Ni atoms and four S atoms, occupying the 2*c* (0.0, 0.5, 0.0) and 4*g* (0.1832, 0.1108, 0.0) Wyckoff positions, respectively. Each Ni atom is six-fold coordinated with six S atoms, while each S atom is four-fold coordinated with three Ni atoms and one S atom. The calculated lattice parameters a = 4.60 Å, b = 5.57 Å, c = 3.55 Å, with the bond lengths of $d_{Ni\text{-}S}$ = 2.38 Å and $d_{S\text{-}S}$ = 2.09 Å. We can obtain the P-NiS_2 monolayer by cleaving along the (100) plane.

The pyrite-type bulk NiS_2 [Fig. S1(b)] has a cubic lattice in $Pa\bar{3}$ symmetry with four Ni atoms and eight S atoms, occupying the 4*b* (0.5, 0.5, 0.5) and 8*c* (0.1069, 0.1069, 0.1069) Wyckoff positions, respectively. Each Ni atom is six-fold coordinated with six S atoms, while each S atom is four-fold coordinated with three Ni atoms and one S atom. The calculated lattice parameters $a = b = c$ = 5.62 Å, with the bond lengths of $d_{Ni\text{-}S}$ = 2.37 Å and $d_{S\text{-}S}$ = 2.08 Å. The bulk NiS_2 is generally considered to be pyrite-type structure.[1-5] We can obtain the O-NiS_2 monolayer by cleaving along the (001) plane.

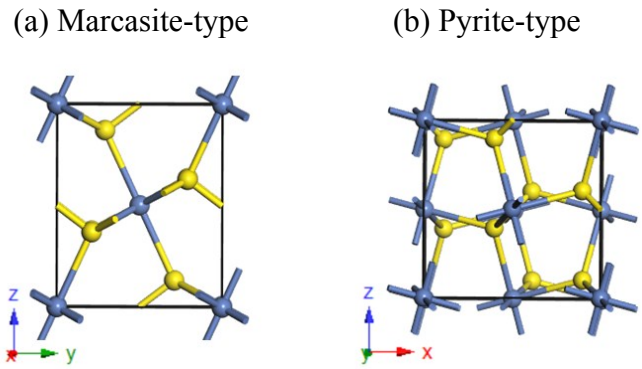

Fig. S1: The bulk structures of (a) marcasite-type NiS_2 and (b) pyrite-type NiS_2. The unit cell is marked by black lines. The blue and yellow balls represent the Ni and S atoms, respectively.

(2) The monolayer structures of O-, T- and H-NiS_2 [6-10]

The O-NiS_2 monolayer [Fig. S2(a)] has a monoclinic lattice in $P2_1/c$ symmetry with two Ni atoms and four S atoms, occupying the 2*b* (0.0, 0.0, 0.5) and 4*e* (0.1166,

0.3762, 0.4713) Wyckoff positions, respectively. Each Ni atom is four-fold coordinated with four S atoms, while each S atom is three-fold coordinated with two Ni atoms and one S atom, forming an intriguing pentagonal ring network known as the Cairo pentagonal tiling. The calculated lattice parameters a = 5.22 Å, b = 5.33 Å, the buckling height h = 0.57 Å, with the bond lengths of $d_{Ni\text{-}S}$ = 2.17, 2.18 Å and $d_{S\text{-}S}$ = 2.13 Å.

The T-NiS_2 monolayer [Fig. S2(b)] has a trigonal lattice in $P\bar{3}m1$ symmetry with one Ni atom and two S atoms, occupying the 1b (0.0, 0.0, 0.5) and 2d (0.3333, 0.6667, 0.5583) Wyckoff positions, respectively. Each Ni atom is six-fold coordinated with six S atoms, while each S atom is three-fold coordinated with three Ni atoms. The calculated lattice parameters a = b = 3.35 Å, the buckling height h = 1.17 Å, with the bond lengths of $d_{Ni\text{-}S}$ = 2.26 Å and $d_{S\text{-}S}$ = 3.03 Å.

The H-NiS_2 monolayer [Fig. S2(c)] has a hexagonal lattice in $P\bar{6}m2$ symmetry with one Ni atom and two S atoms, occupying the 1d (0.3333, 0.6667, 0.5000) and 2g (0.0000, 0.0000, 0.4474) Wyckoff positions, respectively. Each Ni atom is six-fold coordinated with six S atoms, while each S atom is three-fold coordinated with three Ni atoms. The calculated lattice parameters a = b = 3.54 Å, the buckling height h = 1.05 Å, with the bond lengths of $d_{Ni\text{-}S}$ = 2.30 Å and $d_{S\text{-}S}$ = 2.10 Å.

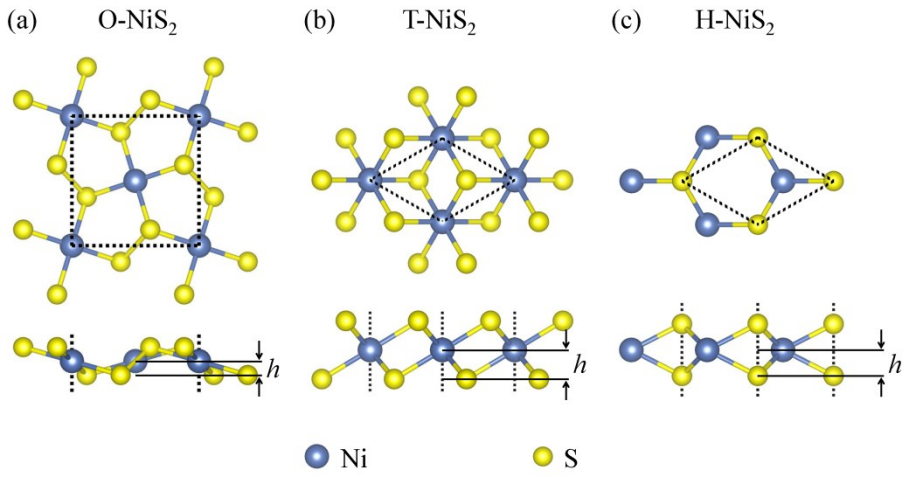

Fig. S2: Top and side views of (a) O-NiS_2 monolayer in $P2_1/c$ symmetry, (b) T-NiS_2 monolayer in $P\bar{3}m1$ symmetry, and (c) H-NiS_2 monolayer in $P\bar{6}m2$ symmetry. The unit cell is marked by black dashed lines. h is the buckling height. The blue and yellow

balls represent the Ni and S atoms, respectively.

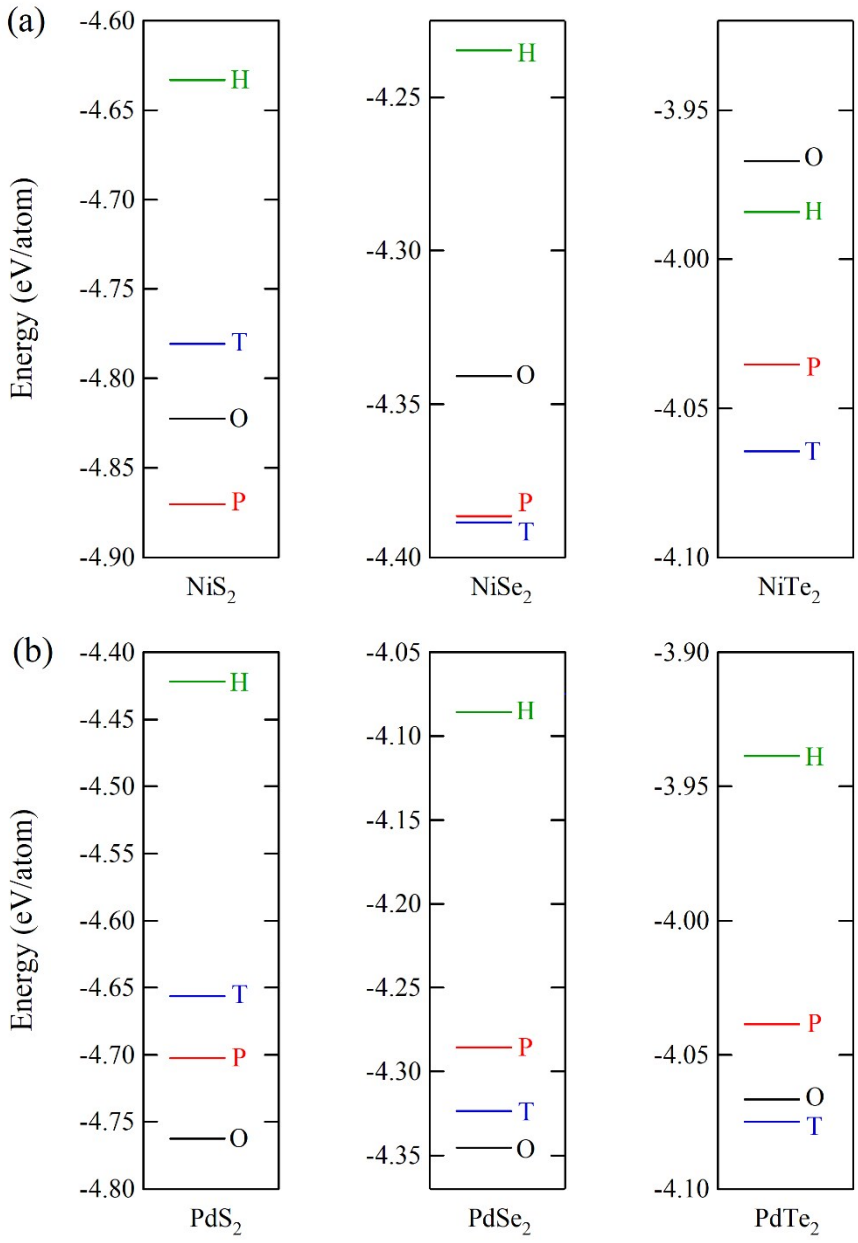

Fig. S3: Energy per atom for (a) NiX_2 and (b) PdX_2 (X = S, Se, Te) monolayers in P-O-, T- and H-structures.

(3) Total energy per atom for NiX_2 and PdX_2 (X = S, Se, Te) monolayers

Fig. S3(a) presents the total energy per atom for P-NiX_2 (X = S, Se, Te) pentagonal network structures (red) in comparison with those for O-, T- and H-NiX_2 monolayers. For NiS_2, the energetic stability sequence is estimated to be: H-NiS_2 < T-NiS_2 < O-NiS_2 < P-NiS_2; for $NiSe_2$, the energetic stability sequence is estimated to be: H-$NiSe_2$

< O-$NiSe_2$ < P-$NiSe_2$ < T-$NiSe_2$; and for $NiTe_2$, the energetic stability sequence is estimated to be: O-$NiTe_2$ < H-$NiTe_2$ < P-$NiTe_2$ < T-$NiTe_2$.

Fig. S3(b) presents the total energy per atom for P-PdX_2 (X = S, Se, Te) pentagonal network structures (red) in comparison with those for O-, T- and H-PdX_2 monolayers. For PdS_2, the energetic stability sequence is estimated to be: H-PdS_2 < T-PdS_2 < P-PdS_2 < O-PdS_2; for $PdSe_2$, the energetic stability sequence is estimated to be: H-$PdSe_2$ < P-$PdSe_2$ < T-$PdSe_2$ < O-$PdSe_2$; and for $PdTe_2$, the energetic stability sequence is estimated to be: H-$PdTe_2$ < P-$PdTe_2$ < O-$PdTe_2$ < T-$PdTe_2$.

It is found that, for pentagonal network structure, the P-NiX_2 is always more favourable in energy than the O-NiX_2, while the O-PdX_2 is always more favourable in energy than the P-PdX_2 is. If we consider all four possible structures, the T-structure becomes more stable in $NiSe_2$, $NiTe_2$, and $PdTe_2$ monolayers. Experimentally, mutilayer O-$PdSe_2$,[11] T-$NiSe_2$,[12] T-$NiTe_2$,[13] and T-$PdTe_2$[14] have been successfully synthesized, which are in good agreement with our calculated results shown in Fig. S3.

References

[1] J. Yin, Y. Li, F. Lv, M. Lu, K. Sun, W. Wang, L. Wang, F. Cheng, Y. Li, P. Xi and S. Guo, *Adv. Mater.*, 2017, **29**, 1704681.

[2] N. Jiang, Q. Tang, M. Sheng, B. You, D.-E. Jiang and Y. Sun, *Catal. Sci. Technol.*, 2016, **6**, 1077-1084.

[3] T. Wang, X. Guo, J. Zhang, W. Xiao, P. Xi, S. Peng and D. Gao, *J. Mater. Chem. A*, 2019, **7**, 4971-4976.

[4] R. L. Kautz, M. S. Dresselhaus, D. Adler and A. Linz, *Phys. Rev. B*, 1972, **6**, 2078-2082.

[5] C. Schuster, M. Gatti and A. Rubio, *Eur. Phys. J. B*, 2012, **85**, 325.

[6] W. Xiong, K. Huang and S. Yuan, *J. Mater. Chem. C*, 2019, **7**, 13518-13525.

[7] H. Yang, Y. Li, Z. Yang, X. Shi, Z. Lin, R. Guo, L. Xu, H. Qu and S. Zhang, *Vacuum*, 2020, **174**, 109176.

[8] C. Ataca, H. Sahin and S. Ciraci, *J. Phys. Chem. C*, 2012, **116**, 8983-8999.

[9] P. Miró, M. Ghorbani-Asl and T. Heine, *Angew. Chem. Int. Ed.*, 2014, **53**, 3015-3018.

[10] J. A. Reyes-Retana and F. Cervantes-Sodi, *Sci. Rep.*, 2016, **6**, 24093.

[11] A. D. Oyedele, S. Yang, L. Liang, A. A. Puretzky, K. Wang, J. Zhang, P. Yu, P. R. Pudasaini, A. W. Ghosh, Z. Liu, C. M. Rouleau, B. G. Sumpter, M. F. Chisholm, W. Zhou, P. D. Rack, D. B. Geohegan and K. Xiao, *J. Am. Chem. Soc.*, 2017, **139**, 14090-14097.

[12] Y. Shao, S. Song, X. Wu, J. Qi, H. Lu, C. Liu, S. Zhu, Z. Liu, J. Wang, D. Shi, S. Du, Y. Wang and H.-J. Gao, *Appl. Phys. Let*t., 2017, **111**, 113107.

[13] B. Zhao, W. Dang, Y. Liu, B. Li, J. Li, J. Luo, Z. Zhang, R. Wu, H. Ma, G. Sun, Y. Huang, X. D. Duan and X. F. Duan, *J. Am. Chem. Soc.*, 2018, **140**, 14217-14223.

[14] E. Li, R.-Z. Zhang, H. Li, C. Liu, G. Li, J.-O. Wang, T. Qian, H. Ding, Y.-Y. Zhang, S.-X. Du, X. Lin and H.-J. Gao, *Chin. Phys. B*, 2018, **27**, 086804.